Nano Energy 93 (2022) 106813

Contents lists available at ScienceDirect

Nano Energy

journal homepage: www.elsevier.com/locate/nanoen

Single atom surface engineering: A new strategy to boost electrochemical activities of Pt catalysts

Lei Zhang [a,b,1], Qi Wang [c,1], Lulu Li [d,e,1], Mohammad Norouzi Banis [b], Junjie Li [b], Keegan Adair [b], Yipeng Sun [b], Ruying Li [b], Zhi-Jian Zhao [d,e,**], Meng Gu [c,*], Xueliang Sun [b,*]

[a] College of Chemistry and Environmental Engineering, Shenzhen University, Shenzhen 518060, PR China
[b] Department of Mechanical and Materials Engineering, The University of Western Ontario, London, ON N6A 5B9, Canada
[c] Department of Materials Science and Engineering, Southern University of Science and Technology, Shenzhen 518055, PR China
[d] Key Laboratory for Green Chemical Technology of Ministry of Education, School of Chemical Engineering and Technology, Tianjin University, Tianjin 300072, PR China
[e] Collaborative Innovation Center of Chemical Science and Engineering (Tianjin), Tianjin 300072, PR China

ARTICLE INFO

Keywords:
Single atom
Surface engineering
Electrochemical reactions
Atomic layer deposition
DFT calculations

ABSTRACT

Pt-based catalysts are widely applied in several catalytic electrochemical reactions for energy storage and conversion. The improvement of specific activity of Pt is typically achieved by introducing the transition metal to obtain the alloy structure. Different from the traditional alloy structure, herein, we report Pt catalyst modified with Co single atoms obtained by atomic layer deposition (ALD). The as-prepared catalysts show much higher mass activity and excellent stability compared to commercial Pt/C catalysts towards the hydrogen evolution reaction (HER) and oxygen reduction reaction (ORR). The atomic resolution TEM images and X-ray absorption spectroscopy (XAS) indicate the formation of atomically dispersed Co on Pt. First principle calculations reveal that the Co atom affects the electronic structure of the Pt catalysts, which resulted in the high HER and ORR performance. This work provides a new approach for the rational design of highly active and stable Pt-based catalysts, which hold great potential for application in various catalytic reactions.

1. Introduction

Pt-based catalysts have wide applications in several industrial areas due to their great electrochemical performance [1–5]. However, the widespread application of Pt is significantly hindered by its low abundance, limited supplies, and ever increasing price. Accordingly, optimizing the mass activity of Pt nanocatalysts is of great concern for minimizing the cost and achieving broader commercialization of Pt. Various methods have been developed for improving two key factors of Pt catalysts; the utilization efficiency and specific activity [6–9]. The improvement of Pt specific activity can be achieved by introducing transition metals to tune the surface electronic structure and atomic coordination. Compared with pure Pt catalysts, Pt-based multi-metallic nanocatalysts have shown great promise in enhancing the ORR [10–15] and HER [16–18] activities due to their intrinsic ligand and geometric effects. In addition to the alloy structure, it is found that the single atom-modified Pt exhibits extremely high activity compared with pure Pt and Pt-based alloy structures [19,20]. For example, Li and co-workers created Ni single atom-modified Pt nanowires through an electrochemical dealloying approach [20]. However, the aforementioned method is limited by the accuracy control of dealloying process, and it is not suitable for potential industrial application. Therefore, it remains a great challenge to develop a new strategy to obtain Pt-based catalysts with single atom modifications that can achieve good performance.

As the electrocatalytic process occurs on the surface of the catalysts, the modification of surface structure can effectively change the catalytic activity compared to the bulk part. ALD is a powerful tool to engineer the surface structure of Pt catalysts, as it can enable precisely control over the deposition of single atoms and nanoclusters [21,22]. In 2013, our group firstly reported a practical synthesis method to fabricate Pt

* Corresponding authors.
** Corresponding author at: Key Laboratory for Green Chemical Technology of Ministry of Education, School of Chemical Engineering and Technology, Tianjin University, Tianjin 300072, PR China.
E-mail addresses: zjzhao@tju.edu.cn (Z.-J. Zhao), gum@sustech.edu.cn (M. Gu), xsun@eng.uwo.ca (X. Sun).
[1] These authors contributed equally to this work.

https://doi.org/10.1016/j.nanoen.2021.106813
Received 1 October 2020; Received in revised form 30 November 2021; Accepted 5 December 2021
Available online 8 December 2021

single atoms on graphene nanosheets by the ALD [23]. The as-prepared Pt single atoms (SA) exhibit greatly enhanced electrochemical activities compared with commercial Pt/C catalysts. The preparation procedure of Pt SA can also be applied for the deposition of other metals. It can be expected that the deposition of single atomic transition metals will further improve the activity of Pt catalysts.

Herein, for the first time, we successfully prepared Co SA-modified Pt nanoparticles (NPs) on nitrogen-doped carbon nanotubes (NCNT) through an ALD process. The detailed structure of the Co SA-modified Pt NPs has been investigated by scanning transmission electron microscopy (STEM), X-ray absorption near edge structure (XANES) and extended X-ray absorption fine structure (EXAFS). The as-prepared Co SA-modified Pt NPs showed much higher catalytic activity and stability compared to commercial Pt/C catalysts for both HER and ORR. Density functional theory (DFT) calculation results indicated that the Co atom affects the electronic structure of the Pt catalysts, which leads to the high HER and ORR performance.

2. Results and discussion

2.1. ALD preparation and characterization of Co SA-modified Pt NPs

Fig. 1a shows the synthesis route for Co SA-modified Pt NPs on NCNT with ALD. NCNTs with an average diameter of 100 nm were prepared by

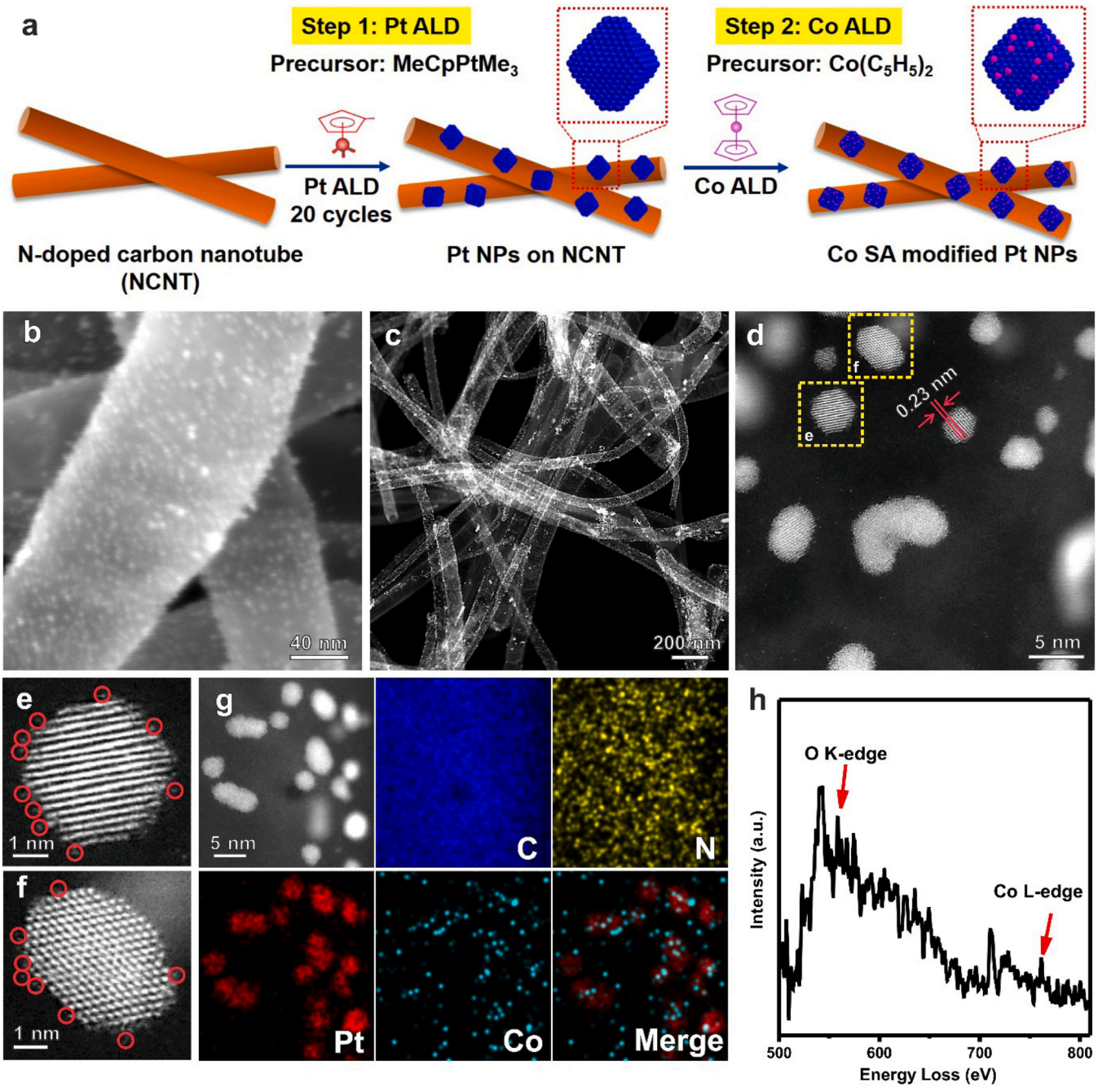

Fig. 1. (a) A schematic illustration showing the preparation process of the Co SA-modified Pt NP catalysts. (b, c) Typical SEM and TEM image of the Co SA modified Pt NPs. (d) Aberration-corrected HAADF-STEM images of Co SA modified Pt NPs catalysts. (e, f) Two individual particles, showing the formation of Co SAs on Pt particles. (g) High resolution HAADF-STEM image and corresponding HAADF-STEM-EDS elemental mapping of Co SA modofied Pt NPs catalysts. (h) EELS spectrum of Co SA modofied Pt NPs catalysts.

ultrasonic spray pyrolysis as outlined previously [24]. Pt NPs were deposited onto the surface of NCNTs through an ALD process by using trimethyl(methylcyclopentadienyl)-platinum (IV) ($MeCpPtMe_3$) and O_2 as the precursors with a nitrogen (99.9995%) purge gas. As shown in Fig. S1, the SEM images indicated that Pt NPs are successfully deposited onto the substrates after 20 Pt ALD cycles. Due to the N-doped sites on NCNT, the Pt atoms can be deposited onto NCNT more easily compared with that on graphene structure. The as-prepared NCNT-Pt catalyst has also been characterized by TEM. As shown in the typical low-resolution TEM image, the Pt NPs are well dispersed on the NCNT substrates (Fig. S2a). The high-resolution TEM image clearly shows uniform Pt particles formed and the surface of the NPs is smooth (Fig. S2b). The periodic fringe spaces are confirmed to be 0.22 nm, which agree well with the d values for the (111) of Pt.

Further modification of the catalyst was conducted by deposition of Co SAs on Pt NPs by ALD using bis(ethylcyclopentadienyl)cobalt(II) as precursor. The typical SEM and HAADF-STEM images show that the size of Pt NPs is not changed after the deposition of Co (Fig. 1b and c). The (111) spacing of Co SA-modified Pt NPs is also found to be 0.23 nm (Fig. 1d). The high-resolution HAADF-STEM images clearly show that the surface of Pt NPs become rough, indicating the formation of isolated Co atoms formed on Pt NPs (Fig. 1e and f; Fig. S3). Furthermore, HAADF-STEM-EDS spectroscopy mapping profiles shown in Fig. S4 clearly reveal the homogeneous distribution of C, N, Pt and Co elements on the NCNTs. In addition, the Energy-dispersive X-ray spectroscopy (EDX) elemental mapping (Fig. 1g) reveals that most of the Co atoms are sparsely deposited on the Pt NPs. The EELS spectrum of Co SA-modified Pt NPs catalysts also show a weak Co signal (Fig. 1h), which indicates the successful ALD deposition of Co atoms. The inductively coupled plasma optical emission spectrometer (ICP-OES) results showed that the loading of the Pt and Co loadings on NCNT are 14 and 0.9 wt%, respectively.

2.2. X-ray absorption fine structure of Co SA-modified Pt NPs

To further investigate the effect of Co SA on Pt structures, we carried out XANES and EXAFS measurements to study the electronic environment of Pt and Co in the Co-modified Pt catalysts (Fig. 2). Fig. 2a and b

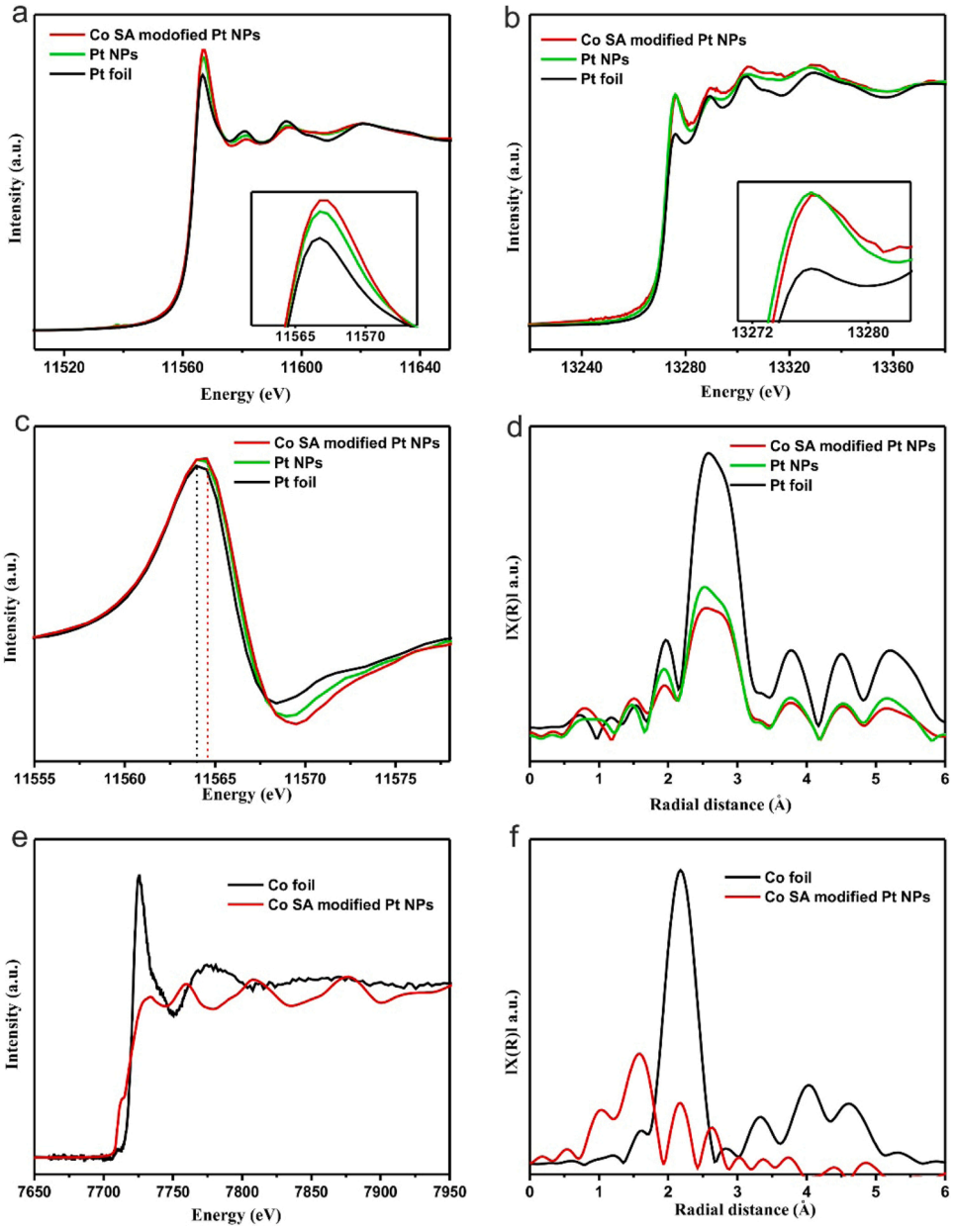

Fig. 2. X-ray absorption studies of the Co SA-modified Pt NPs and regular Pt NPs in comparison with Pt foil. (a, b) The normalized XANES spectra at the Pt L_3-edge and L_2-edge of the Co SA modified Pt NPs, regular Pt NPs and Pt foil. (c) The first derivative of the XANES spectrum at Pt L_3 edge. (d) Corresponding K_3-weighted magnitude of Fourier transform spectra from EXAFS of Co SA modified Pt NPs, Pt NPs and Pt foil. (e) The normalized XANES spectra at the Co K-edge of the Co SA modified Pt NPs, regular Pt NPs and Pt foil. (f) Corresponding K_3-weighted magnitude of Fourier transform spectra from Co K-edge of Co SA modified Pt NPs and Co foil.

shows the normalized XANES spectra at the Pt L_3 and L_2 edges, respectively. Detailed examination of the spectra was conducted by qualitative and quantitative analysis of the Pt L_2 and L_3 edges white lines (WLs, the sharp intense peak lead by the rising absorption edge) [25]. It is apparent that, with the exception of Pt foil, which has an intense L_3-edge WL and a very weak L_2-edge WL due to the large spin orbit coupling of the 5d and an even distribution of the 5d $_{5/2}$ and 5d$_{3/2}$ densities of states just above the fermi level in metallic Pt, both the Pt NPs and Co modified Pt catalysts exhibit substantial WL intensity at both edges. In addition, the Co modified Pt catalysts appear to have the most intense WL compare to Pt NPs and Pt foil. It has been shown that the area under the WL peak of $L_{2,3}$-edge x-ray absorption spectra of the Pt metal is directly related to the unoccupied density of states of the Pt 5d orbitals. An increase in the $L_{2,3}$-edge WL intensity indicates a decrease in the number of electrons in the occupied d band. In addition, a small positive shift in the threshold energy E_0 can be observed for Co-modified Pt catalysts compared to Pt NPs and Pt foil. The detailed E_0 position can be determined by the first derivative of the XANES spectrum at the Pt L_3 edge (Fig. 2c). Among the three samples, the E_0 for Co modified Pt catalysts is 11,564.5 eV, which is slightly higher than that of 11564 eV of Pt NPs. This result suggests that Pt experiences a more oxidized environment when modified by Co SAs. To further explore the implication of the unoccupied densities of 5d states in Pt, quantitative WL intensity analysis was conducted based on a reported method to determine the occupancy of the 5d states in each sample. The Pt L_3- and Pt L_2-edge threshold and WL parameters are summarized in Table 1. From the analysis, the Co-modified Pt catalysts have the highest total unoccupied density of states of Pt 5d character (0.85), while the Pt foil sample had the lowest of 0.67. It has been demonstrated in literature that the vacant D-orbitals of Pt atoms play a vital role in the activity of catalysts [20,22,26].

Furthermore, to study the local structure environment of Pt, the EXAFS spectrum was studied. The magnitude of Fourier transforms (FT) of the Pt EXAFS for different samples were plotted in Fig. 2d. The EXAFS R space curve fitting attributes the FT magnitude peak at around 2.6 Å to the Pt–Pt or Pt-Co bonding. When we carefully compare the EXAFS peaks of Pt NPs and Co modified Pt NPs, we found that the peak position slightly shifted from 2.58 Å to 2.51 Å. The peaks are fitted to quantitatively obtain the coordination number (CN) and bonding length of Pt-Pt (Fig. S5 and Table S1). As shown in Table S1, the Pt-Pt for the Pt NPs and Co-modified Pt NPs have relatively lower CN (9.4 and 8.7) relative to Pt foil (12) due to the presence of nano-sized Pt nanoparticles on the substrates. In addition, we found the bonding distance of Pt-Pt for the Co-modified Pt NPs decreased to 2.73 Å, which is also lower than that of Pt foil (2.76 Å). This result indicated that, with the deposition of Co atoms on Pt, the Pt electronic structure was tuned. The formation of Pt-Co bond (3.04 Å) caused the reconstruction of Pt surfaces, reducing the bond distance of Pt-Pt bond to 2.73 Å. This result also provided the evidence for the formation of Pt-Co bond on Pt surface [27]. It should be mentioned that a very small Pt-Co bond (CN=0.1) is simulated, which also indicates that Co is deposited on the Pt surface.

X-ray absorption spectroscopy (XAS) was also used to study the Co local electronic structure of the Co-modified Pt NPs (Fig. 2e). Qualitative examination of the Co K-edge XANES spectra whiteline clearly shows a shift in edge position to higher energies compared to Co foil, indicating the partial oxidation of Co on Pt surface using the ALD process. The EXAFS of the Co K-edge was also studied in detail. The Fourier transforms of the EXAFS region for Co-modified Pt NPs and Co foil are plotted in Fig. 2f. The Co-modified Pt NPs exhibited an obvious Co-O peak at around 1.6 Å. Two different types of Co-O, Co(II)-O and Co(III)-O, might exist on the Co modified Pt catalysts [28]. A relative weak peak was observed at around 2.3 Å, which can be attributed to the Co-M (M=Co or Pt) bond. The atomic resolution TEM images showed the formation of Co single atoms on Pt. In addition, the corresponding fitting results about Pt L3 edge and Co K edge also indicated the peak at 2.2 Å belonged to Co-Pt peak instead of Co-Co peak. The detailed peak attribution is provided in Fig. S6 and the detailed fitted parameters are summarized in Table S2. As shown in Fig. S6, the R space curve fitting agrees well with the experimental data. From the Co K-edge R space fitting results, the Co atoms have the CN of 0.8 for Co-Pt, also suggesting the formation of Co single atoms on Pt surface. In addition, the fitting bond length of Co-Pt is 2.83 Å, which is close to that of Pt-Co (3.04 Å). The relatively longer distance of Co-Pt bond is due to the formation of Co-O bond during the ALD process.

2.3. Electrocatalytic performance of Co SA-modified Pt NPs

The HER activity of the Co SA-modified Pt NPs was firstly measured in comparison to the Pt NPs and commercial Pt/C catalysts by conducting linear sweep voltammetry measurements in 0.5 M H_2SO_4 at room temperature (Fig. 3a–c). The polarization curves show that the Co SA-modified Pt NPs exhibit better HER performance compared with Pt NPs and commercial Pt/C, as shown in Fig. 3a. The specific activity for each catalyst is calculated from the polarization curves by normalizing the current with the geometric area of the electrode (Fig. S7). The Co SA modified Pt NPs exhibited a current density of 158 mA/cm^2 at an overpotential of 0.07 V. When normalized to the metal loading, the mass HER activities for the Co SA-modified Pt NPs at an overpotential of 0.07 V is 11.5 A mg^{-1}(Fig. 3b), which is 3.5 and 16.4 times greater than that of the Pt NPs (3.3 A mg^{-1}) and Pt/C catalysts (0.7 A mg^{-1}), respectively. In addition, we prepared the Pt NPs with 5 cycles Co ALD deposition (5ALD Co-Pt NPs/NCNT) and tested the electrochemical performance. As shown in Fig. S8, the mass HER activity reduced to 4.3 A mg^{-1} at the overpotential of 0.07 V, which indicated that increasing the Co deposition on Pt catalysts might cover the active sites on Pt surface, thus affect the electrochemical performance of the catalysts. To evaluate the durability of the as-prepared Co SA modified Pt catalysts, accelerated degradation tests (ADTs) were adopted between +0.4 and −0.15 V (versus RHE) at 100 mV s^{-1} for 5000 cyclic voltammetry sweeps. As exhibited in Fig. 3c, the polarization curve of Co SA modified Pt NPs after 5000 cycles retained a similar performance to the initial test, resulting in a loss of only 17% of its initial current density at an overpotential of 0.07 V (Fig. 3c). Furthermore, we examined the HER performance of Co SA-modified Pt NPs, Pt NPs and commercial Pt/C catalysts in 1.0 M KOH at room temperature(Fig. 3d–f). Fig. S9 reveals the current densities in alkaline solution were 32.7, 13.7 and 17.8 mA/

Table 1
Pt $L_{3,2}$-edge threshold and whiteline (WL) parameters.

Sample	Pt L_3 edge WL			Pt L_2 edge WL			$h_{5/2}$	$h_{3/2}$	Total
	E_0 (eV)[a]	E_{Peak} (eV)[b]	ΔA_3[c]	E_0 (eV)	E_{Peak} (eV)	ΔA_3			
Pt foil	11564	11,566.7	6.46	13,273	13,276.1	1.47	0.61	0.07	0.67
Pt NPs on NCNT	11564	11,566.7	7.10	13,273	13,276.1	3.53	0.64	0.16	0.81
Co SA modified Pt NPs	11,564.5	11,567.0	7.15	13,273.3	13,276.3	4.39	0.65	0.20	0.85

[a] Position of the first inflection point of the edge jump for the corresponding Pt L_3 edge.
[b] Peak position.
[c] Area under the difference curve for normalized edge jump, the normalized edge jump for the Pt L_3 and L_2 edge corresponds to a value of 2.5 × 10^3 cm^{-1} and 1.16 × 10^3 cm^{-1}, respectively.

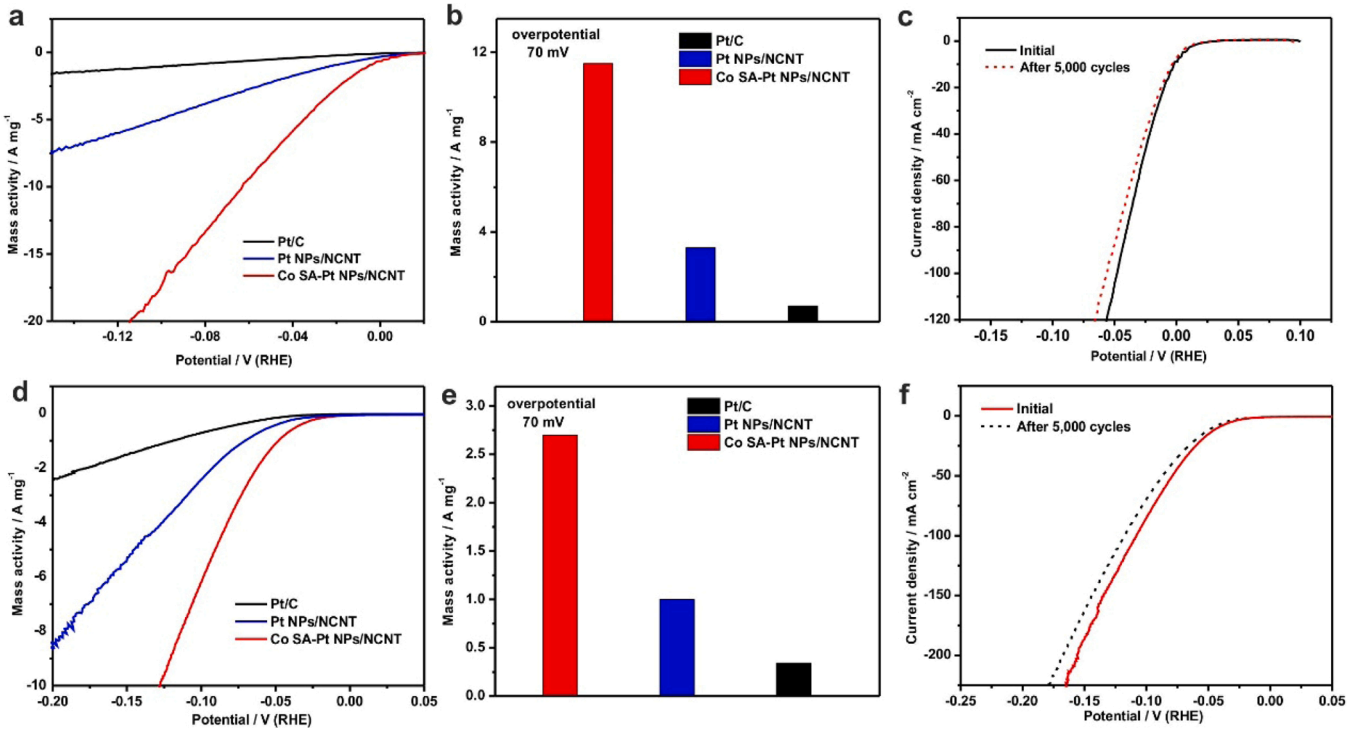

Fig. 3. (a) The HER polarization curves recorded on Co SA modified Pt NPs, regular Pt NPs and commercial Pt/C catalysts in 0.5 M H_2SO_4 at room temperature. (b) The current mass activity at −0.07 V in acid solution. (c) Durability measurement of the Co SA modified Pt NPs catalysts. (d) The HER polarization curves recorded on Co SA modified Pt NPs, regular Pt NPs and commercial Pt/C catalysts in 1.0 M KOH at room temperature. (e) The current mass activity at −0.07 V in alkaline solution. (f) Durability measurement of the Co SA modified Pt NPs catalysts in alkaline solution.

cm^2 on the Co SA modified Pt NPs, Pt NPs and commercial Pt/C catalysts at −0.07 V, respectively. In addition, the Co SA-modified Pt NPs still exhibited the best mass activity (2.7 A mg^{-1} at the overpotential of 0.07 V) among these three catalysts (Fig. 3e). After 5000 cycles ADT test, the Co SA modified Pt NPs showed only a loss of only 7% of its initial current density at an overpotential of 0.07 V in 1.0 M KOH solution (Fig. 3 f). It can be found that the electrocatalytic abilities of the Co SA-modified Pt NPs exhibited superior HER performance in both acid and alkaline solution compared to the commercial Pt/C catalyst.

We also evaluated the ORR performance of the Co SA-modified Pt NPs, Pt NPs and commercial Pt/C catalysts. Cyclic voltammograms (CV) were recorded in 0.10 M aqueous $HClO_4$ at a scanning rate of 50 mV•s^{-1}(Fig. 4a). The ECSA for the Co SA modified Pt NPs, Pt NPs and Pt/C catalysts were 63.6, 70.3 and 34.3 m^2/g, respectively. The polarization ORR curve showed that the Co SA modified Pt NPs exhibited better activity than that of the Pt NPs and Pt/C (40%) (Fig. 4b). In order to compare the activity for different catalysts, we normalized the kinetic current to the Pt mass (Fig. 4c and d). The kinetic current density (j_k) was derived from the Koutecky-Levich equation [29]. As shown in Fig. 4e, the Co SA modified Pt NPs exhibited greatly improved specific activity, with $j_{k,\ specific}$ values of 0.77 mA /cm^2 based on the ECSA at 0.9 V vs. RHE, which was 1.5 and 3.8 times greater than that of the Pt NPs (0.51 mA/cm^2) and Pt/C catalyst (0.20 mA/cm^2), respectively. The mass activities of the Co SA modified Pt NPs, Pt NPs and Pt/C catalysts were 0.49, 0.26 and 0.11 A/mg, respectively, showing similar trends to that of the specific activities. As shown in Fig. 4f, the Co SA-modified NPs had obviously improved $j_{k,\ mass}$ relative to the Pt/C catalyst. These results indicate that the shortened Pt-Pt bond distance by the Co modification can greatly improve the performance of the catalysts for ORR. It should be pointed that the increase of Co ALD cycles also affected the ORR performance of the catalysts. As shown in Fig. S10a, the ECSA of the catalysts significantly reduced due to the high coverage of Co on Pt surface. In addition, the mass activity reduced to 0.17 A/mg (Fig. S10b–d), indicating the significant role of Co single atom modification. We also tested the long-term stability of the catalysts through ADT between +0.6 and +1.1 V (vs. RHE) at 100 mV s^{-1} for 10, 000 cyclic voltammetry sweeps. For the mass ORR activities at 0.9 V, the Co SA-modified Pt NPs, which achieved the best activity towards ORR, only showed a 20.8% loss in mass activity after 10,000 cycles (Fig. S11). In addition, the TEM images of post-testing samples indicated that the particles are still well-dispersed on the NCNT (Fig. S12a and b). EDX mapping indicated that Co and Pt are not dissolved in the solution during the ADT test (Fig. S12c). These results indicate that the Co SA-modified Pt NPs exhibit good durability.

2.4. The enhanced mechanism elucidated by DFT calculations

Density functional theory (DFT) calculations were conducted to further elucidate the mechanism behind the improved HER and ORR performance enabled by Co SA-modified Pt NPs. Pt (111) and Co SA modified Pt (111) were used for the calculation models (Fig. 5a) based on the HAADF-STEM and EXAFS results discussed above (Fig. 1, Tables S1 and S2). The hydrogen adsorption free energies (ΔG_{H^*}) and all potential adsorption sites for hydrogen are first calculated to probe the activity of HER. Furthermore, in order to get simulation results closer to the real reaction conditions, a volcano-type kinetic model, which expresses the experimental exchange current i_0 as a function of ΔG_{H^*} (Fig. 5b) was employed [30]. An obvious volcano plot is shown in Fig. 5b. On the left part of the volcano plot, hydrogen bond energy is strong, leading to the difficulty in H_2 generation. On the contrary, the right part of the volcano means proton transfer becomes rough, which result in the weak hydrogen bond. Generally, hydrogen-binding on Pt (111) is strong and concentrated on the left side of the volcano. In addition, the calculations for the Co SA-modified Pt(111) show that ΔG_{H^*} decreases to region of optimal HER activity. Moreover, the d band center of Pt(111) (−1.94 eV) and Co SA-modified Pt(111) (−2.04 eV, −2.30 eV) (Fig. S13) also demonstrate that Co SA species can modify the electronic structure of the surface Pt atoms by lowering of the d band.

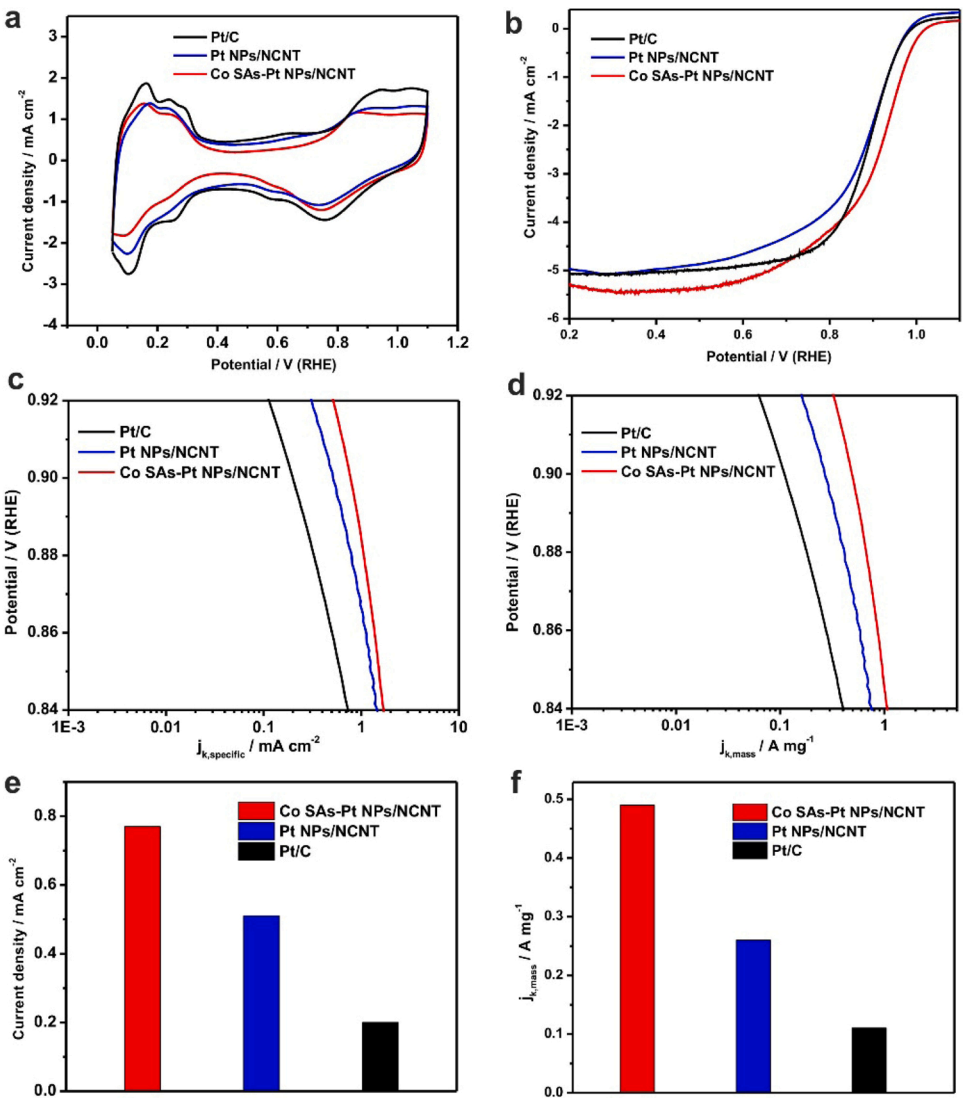

Fig. 4. (a) The CV curves in the potential region from 0.05 to 1.10 V recorded on Co SA modified Pt NPs, regular Pt NPs and commercial Pt/C catalysts. (b) ORR polarization curves of the Co SA modified Pt NPs in comparison with regular Pt NPs and commercial Pt/C catalysts. The current densities were normalized to the geometric area of the RDE (0.196 cm^2). (c) Specific and (d) mass activities given as kinetic current densities (j_k) normalized against the ECSAs of the catalysts and the mass of Pt, respectively. (e, f) Specific and mass activities at 0.9 V_{RHE} of the catalysts.

Therefore, the adsorption strength of hydrogen is weakened, leading to the optimal HER activity.

To further explore the ORR performance between Pt(111) and Co SA modified Pt(111), theoretical calculations for the reaction mechanism were explored. The free energy diagrams of the ORR on Pt(111) and Co SA modified Pt(111) are shown in Fig. 5c. In the case where the electrode potential is zero ($U = 0$ V), the elementary reactions of ORR on both surfaces are exothermic, and the adsorption of O* and OH* is weakened on Co SA modified Pt(111). Moreover, previous studies [31, 32] on the ORR mechanism indicate that O protonation to OH is the rate-determining step, and thus catalysts with weakly binding oxygen species have better ORR activity. Therefore, the Pt atoms electronically modified by Co SA species are beneficial for the ORR performance. Additionally, when the electrode potential is 1.23 V, OH protonation on Co SA modified Pt(111) is found to be more facile than Pt(111). This further suggests that the Co SA modified Pt(111) could provide more available sites for ORR, which is consistent with the stability of Pt(111) and Co-SA modified Pt(111) found experimentally [33–35].

3. Conclusion

In conclusion, we have successfully synthesized Co SA-modified Pt catalysts on NCNTs by ALD. The obtained Co SA-modified Pt NPs showed significantly improved activity and excellent stability compared to commercial Pt/C catalysts for both HER and ORR. X-ray absorption spectroscopy indicates that the structure model of Co SA-modified Pt NPs contain one Co-Pt bonding configuration. Furthermore, the DFT calculation results reveal that the Co SA-modified Pt(111) show decreased ΔG_{H^*} to the value of the optimal HER activity region. During the ORR process, the adsorption of O* and OH* weakened on Co SA modified Pt(111), which is beneficial for the ORR performance. This work paves a new way for the rational design of bimetallic catalysts, which have great potential for application in various catalytic reactions.

CRediT authorship contribution statement

L. Zhang conceived and designed the experimental work and prepared the manuscript; M. Norouzi Banis, Y. Sun and J. Li helped with ALD characterization; Q. Wang and M. Gu performed STEM characterization; Z.-J. Zhao and L. Li performed the DFT calculations; R. Li, and K. Adair participated in the discussion of the data; X. Sun supervised the overall project. All authors have given approval to the final version of the manuscript.

Declaration of Competing Interest

The authors declare that they have no known competing financial interests or personal relationships that could have appeared to influence

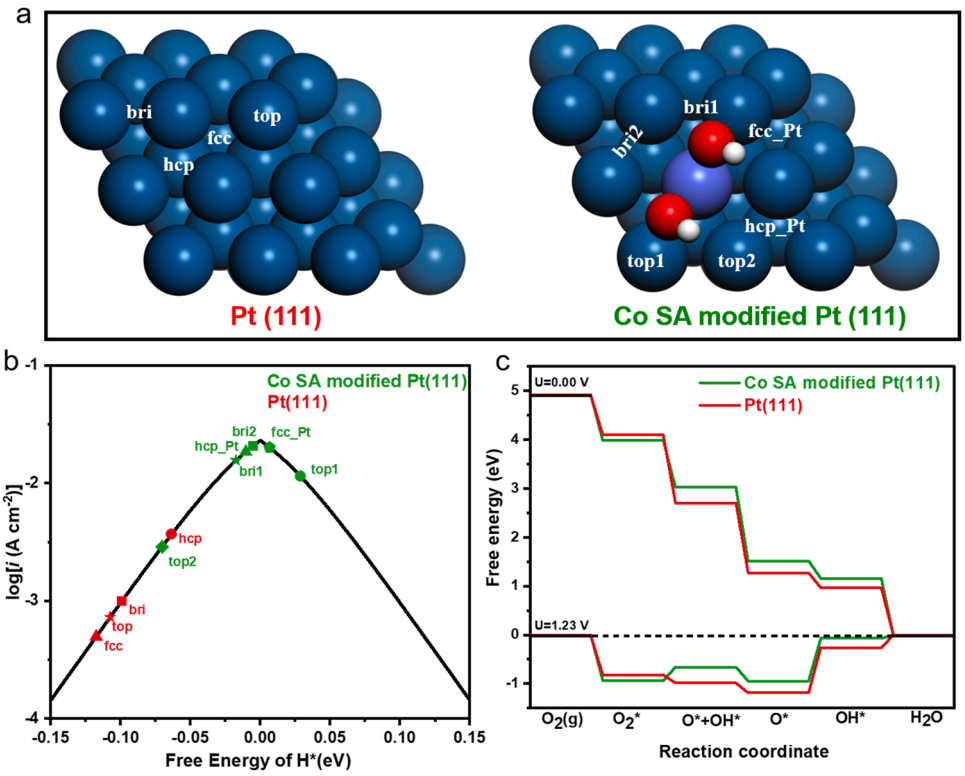

Fig. 5. (a) DFT models of Pt(111) and Co SA modified Pt(111); (b) Exchange current i_0 for HER as a function of *H adsorption free energy for the adsorption sites in Pt(111) and Co SA modified Pt(111); (c) Free energy profiles of ORR on Pt (111) and Co SA modified Pt (111).

the work reported in this paper.

Acknowledgments

This work was supported by the National Natural Science Foundation of China (22075203), Natural Science Foundation of SZU (000002111605), Natural Sciences and Engineering Research Council of Canada (NSERC), Canada Research Chair (CRC) Program, Canada Foundation for Innovation (CFI) and the University of Western Ontario. We also want to acknowledge Canadian Urban Transit Research and Innovation Consortium (CUTRIC) project and Ballard Power Systems Inc.

Appendix A. Supporting information

Supplementary data associated with this article can be found in the online version at doi:10.1016/j.nanoen.2021.106813.

References

[1] N. Tian, Z.Y. Zhou, S.G. Sun, Y. Ding, Z.L. Wang, Synthesis of tetrahexahedral platinum nanocrystals with high-index facets and high electro-oxidation activity, Science 316 (2007) 732–735, https://doi.org/10.1126/science.1140484.

[2] L. Gan, C. Cui, M. Heggen, F. Dionigi, S. Rudi, P. Strasser, Element-specific anisotropic growth of shaped platinum alloy nanocrystals, Science 346 (2014) 1502–1506, https://doi.org/10.1126/science.1261212.

[3] L. Zhang, L.T. Roling, X. Wang, M. Vara, M. Chi, J. Liu, S.I. Choi, J. Park, J. A. Herron, Z. Xie, M. Mavrikakis, Y. Xia, Platinum-based nanocages with subnanometer-thick walls and well-defined, controllable facets, Science 349 (2015) 412–416, https://doi.org/10.1126/science.aab0801.

[4] C. Chen, Y. Kang, Z. Huo, Z. Zhu, W. Huang, H.L. Xin, J.D. Snyder, D. Li, J. A. Herron, M. Mavrikakis, M. Chi, K.L. More, Y. Li, N.M. Markovic, G.A. Somorjai, P. Yang, V.R. Stamenkovic, Highly crystalline multimetallic nanoframes with three-dimensional electrocatalytic surfaces, Science 343 (2014) 1339–1343, https://doi.org/10.1126/science.1249061.

[5] M. Li, Z. Zhao, T. Cheng, A. Fortunelli, C.Y. Chen, R. Yu, Q. Zhang, L. Gu, B. V. Merinov, Z. Lin, E. Zhu, T. Yu, Q. Jia, J. Guo, L. Zhang, W.A. Goddard III, Y. Huang, X. Duan, Ultrafine jagged platinum nanowires enable ultrahigh mass activity for the oxygen reduction reaction, Science 354 (2016) 1414–1419, https://doi.org/10.1126/science.aaf9050.

[6] V.R. Stamenkovic, B.S. Mun, M. Arenz, K.J.J. Mayrhofer, C.A. Lucas, G. Wang, P. N. Ross, N.M. Markovic, Trends in electrocatalysis on extended and nanoscale Pt-bimetallic alloy surfaces, Nat. Mater. 6 (2007) 241–247, https://doi.org/10.1038/nmat1840.

[7] M. Shao, A. Peles, K. Shoemaker, Electrocatalysis on platinum nanoparticles: particle size effect on oxygen reduction reaction activity, Nano Lett. 11 (2011) 3714–3719, https://doi.org/10.1021/nl2017459.

[8] M. Nesselberger, S. Ashton, J.C. Meier, I. Katsounaros, K.J.J. Mayrhofer, M. Arenz, The particle size effect on the oxygen reduction reaction activity of Pt catalysts: influence of electrolyte and relation to single crystal models, J. Am. Chem. Soc. 133 (2011) 17428–17433, https://doi.org/10.1021/ja207016u.

[9] F.A. Bruijn, V.A.T. Dam, G.J.M. Janssen, Durability and degradation issues of PEM fuel cell components, Fuel Cells 8 (2008) 3–22, https://doi.org/10.1002/fuce.200700053.

[10] J. Zhang, H. Yang, J. Fang, S. Zou, Synthesis and oxygen reduction activity of shape-controlled Pt3Ni nanopolyhedra, Nano Lett. 10 (2010) 638–644, https://doi.org/10.1021/nl903717z.

[11] J. Wu, A. Gross, H. Yang, Shape and composition-controlled platinum alloy nanocrystals using carbon monoxide as reducing agent, Nano Lett. 11 (2011) 798–802, https://doi.org/10.1021/nl104094p.

[12] S. Choi, S. Xie, M. Shao, J.H. Odell, N. Lu, H.C. Peng, L. Protsailo, S. Guerrero, J. Park, X. Xia, J. Wang, M.J. Kim, Y. Xia, Synthesis and characterization of 9 nm Pt–Ni octahedra with a record high activity of 3.3 A/mgPt for the oxygen reduction reaction, Nano Lett. 13 (2013) 3420–3425, https://doi.org/10.1021/nl401881z.

[13] C. Cui, L. Gan, M. Heggen, S. Rudi, P. Strasser, Compositional segregation in shaped Pt alloy nanoparticles and their structural behaviour during electrocatalysis, Nat. Mater. 12 (2013) 765–771, https://doi.org/10.1038/nmat3668.

[14] L. Zhang, K. Doyle-Davis, X. Sun, Pt-Based electrocatalysts with high atom utilization efficiency: from nanostructures to single atoms. Energy Environ. Sci. 12 (2019) 492–517. https://doi.org/10.1039/C8EE02939C.

[15] B. Han, C.E. Carlton, A. Kongkanand, R.S. Kukreja, B.R. Theobald, L. Gan, R. O'Malley, P. Strasser, F.T. Wagner, Y. Shao-Horn, Record activity and stability of dealloyed bimetallic catalysts for proton exchange membrane fuel cells. Energy Environ. Sci. 8 (2015) 258–266. https://doi.org/10.1039/C4EE02144D.

[16] P. Wang, X. Zhang, J. Zhang, S. Wan, S. Guo, G. Lu, J. Yao, X. Huang, Precise tuning in platinum-nickel/nickel sulfide interface nanowires for synergistic hydrogen evolution catalysis, Nat. Commun. 8 (2017) 14580, https://doi.org/10.1038/ncomms14580.

[17] Z. Zhao, H. Liu, W. Gao, W. Xue, Z. Liu, J. Huang, X. Pan, Y. Huang, Surface-engineered PtNi-O nanostructure with record-high performance for electrocatalytic hydrogen evolution reaction, J. Am. Chem. Soc. 140 (2018) 9046–9050, https://doi.org/10.1021/jacs.8b04770.

[18] P. Wang, K. Jiang, G. Wang, J. Yao, X. Huang, Phase and interface engineering of platinum–nickel nanowires for efficient electrochemical hydrogen evolution, Angew. Chem. 128 (2016) 13051–13055, https://doi.org/10.1002/ange.201606290.
[19] L. Cao, W. Liu, Q. Luo, R. Yin, B. Wang, J. Weissenrieder, M. Soldemo, H. Yan, Y. Lin, Z. Sun, C. Ma, W. Zhang, S. Chen, H. Wang, Q. Guan, T. Yao, S. Wei, J. Yang, J. Lu, Atomically dispersed iron hydroxide anchored on Pt for preferential oxidation of CO in H2, Nature 565 (2019) 631–635, https://doi.org/10.1038/s41586-018-0869-5.
[20] M. Li, K. Duanmu, C. Wan, T. Cheng, L. Zhang, S. Dai, W. Chen, Z. Zhao, P. Li, H. Fei, Y. Zhu, R. Yu, J. Luo, K. Zang, Z. Lin, M. Ding, J. Huang, H. Sun, J. Guo, X. Pan, W.A. Goddard III, P. Sautet, Y. Huang, X. Duan, Single-atom tailoring of platinum nanocatalysts for high-performance multifunctional electrocatalysis, Nat. Catal. 2 (2019) 495–503, https://doi.org/10.1038/s41929-019-0279-6.
[21] N. Cheng, S. Stambula, D. Wang, M. Banis, J. Liu, A. Riese, B. Xiao, R. Li, T. K. Sham, L. Liu, G. Botton, X. Sun, Platinum single-atom and cluster catalysis of the hydrogen evolution reaction, Nat. Commun. 7 (2016) 13638, https://doi.org/10.1038/ncomms13638.
[22] H. Yan, Y. Lin, H. Wu, W. Zhang, Z. Sun, H. Cheng, W. Liu, C. Wang, J. Li, X. Huang, T. Yao, J. Yang, S. Wei, J. Lu, Bottom-up precise synthesis of stable platinum dimers on graphene, Nat. Commun. 8 (2017) 1070, https://doi.org/10.1038/s41467-017-01259-z.
[23] S.H. Sun, G.X. Zhang, N. Gauquelin, N. Chen, J.G. Zhou, S.L. Yang, W.F. Chen, X. B. Meng, D.S. Geng, M.N. Banis, R. Li, S. Ye, S. Knights, G.A. Botton, T.K. Sham, X. Sun, Single-atom catalysis using Pt/graphene achieved through atomic layer deposition, Sci. Rep. 3 (2013) 1775, https://doi.org/10.1038/srep01775.
[24] L.G. Bulusheva, A.V. Okotrub, A.G. Kurenya, H. Zhang, H. Zhang, X. Chen, H. Song, Electrochemical properties of nitrogen-doped carbon nanotube anode in Li-ion batteries, Carbon 49 (2011) 4013, https://doi.org/10.1016/j.carbon.2011.05.043.
[25] D. Wang, X. Cui, Q. Xiao, Y. Hu, Z. Wang, Y.M. Yiu, T.K. Sham, Electronic behaviour of Au-Pt alloys and the 4f binding energy shift anomaly in Au bimetallics- X-ray spectroscopy studies, AIP Adv. 8 (2018), 065210, https://doi.org/10.1063/1.5027251.
[26] P. Hu, Z. Huang, Z. Amghouz, M. Makkee, F. Xu, F. Kapteijn, A. Dikhtiarenko, Y. Chen, X. Gu, X. Tang, Electronic metal–support interactions in single-atom catalysts, Angew. Chem., Int. Ed. 53 (2014) 3418, https://doi.org/10.1002/ange.201309248.
[27] L.G. Cesar, C. Yang, Z. Lu, Y. Ren, G. Zhang, J.T. Miller, Identification of a Pt3Co surface intermetallic alloy in Pt–Co propane dehydrogenation catalysts, ACS Catal. 9 (2019) 5231, https://doi.org/10.1021/acscatal.9b00549.
[28] M. Ma, Z. Pan, L. Guo, J. Li, Z. Wu, S. Yang, Porous cobalt oxide nanowires: notable improved gas sensing performances, Chin. Sci. Bull. 31 (2012) 4019, https://doi.org/10.1007/s11434-012-5363-0.
[29] H.A. Gasteiger, S.S. Kocha, B. Sompalli, F.T. Wagner, Activity benchmarks and requirements for Pt, Pt-alloy, and non-Pt oxygen reduction catalysts for PEMFCs, Appl. Catal. B 56 (2005) 9, https://doi.org/10.1016/j.apcatb.2004.06.021.
[30] J.K. Nørskov, T. Bligaard, A. Logadottir, J.R. Kitchin, J.G. Chen, S. Pandelov, U. Stimming, Trends in the exchange current for hydrogen evolution, J. Electrochem. Soc. 152 (2005) J23–J26, https://doi.org/10.1149/1.1856988.
[31] L. Ou, S. Chen, Comparative study of oxygen reduction reaction mechanisms on the Pd (111) and Pt (111) surfaces in acid medium by DFT, J. Phys. Chem. C 117 (2013) 1342–1349, https://doi.org/10.1021/jp309094b.
[32] L. Ou, The origin of enhanced electrocatalytic activity of Pt–M (M= Fe, Co, Ni, Cu, and W) alloys in PEM fuel cell cathodes: a DFT computational study, Comput. Theor. Chem. 1048 (2014) 69–76, https://doi.org/10.1016/j.comptc.2014.09.017.
[33] C.H. Cui, H.H. Li, X.J. Liu, M.R. Gao, S.H. Yu, Surface composition and lattice ordering-controlled activity and durability of CuPt electrocatalysts for oxygen reduction reaction, ACS Catal. 2 (2012) 916–924, https://doi.org/10.1021/cs300058c.
[34] N. Hodnik, C. Jeyabharathi, J.C. Meier, A. Kostka, K.L. Phani, A. Rečnik, M. Bele, S. Hočevar, M. Gaberšček, K.J.J. Mayrhofer, Effect of ordering of PtCu3 nanoparticle structure on the activity and stability for the oxygen reduction reaction, Phys. Chem. Chem. Phys. 16 (2014) 13610–13615, https://doi.org/10.1039/C4CP00585F.
[35] K. Li, Y. Li, Y. Wang, F. He, M. Jiao, H. Tang, Z. Wu, The oxygen reduction reaction on Pt (111) and Pt (100) surfaces substituted by subsurface Cu: a theoretical perspective, J. Mater. Chem. A 3 (2015) 11444–11452, https://doi.org/10.1039/C5TA01017A.

Prof. Lei Zhang received his Ph.D. degree in Xiamen University. He was a visiting graduate student at Georgia Institute of Technology in Prof. Younan Xia's group from 2012 to 2014. From 2015–2016, he worked as a Postdoc at Tianjin University. He was a postdoctoral associate with Prof. Xueliang Sun at Western University from 2017 to 2021. From 2021, he is a professor in Shenzhen University. His research interests include the design and synthesis of metal nanomaterials and single atom catalysts for fuel cells.

Qi Wang received his Bachelor in 2011 and Ph.D. in 2017 from Central South University. He's currently doing his postdoctoral research in Dr. Gu's group at Southern University of Science and Technology. His research interests focus on the TEM and structure-property relationship of materials in electrocatalysis.

Lulu Li is currently a Ph.D. candidate in chemical technology at Tianjin University under the supervision of Professor Zhi-Jian Zhao. She received her BS degree in applied chemistry in 2017 from Dalian University of Technology and MS degree in chemical technology in 2019 from Tianjin University. Her research focuses on mechanistic studies of heterogeneous catalyst on electrocatalysis.

Dr. Mohammad Norouzi Banis is a research engineer in Prof. Xueliang (Andy) Sun's group at the University of Western Ontario, Canada. He received his Ph.D. degree in 2013 in Materials Science and Engineering from Western University, on the study of nanostructured low temperature fuel cells and application of x-ray absorption spectroscopy in energy related systems. His current research interests include study of metal ion, metal air and nanocatalysts via in-situ synchrotron-based techniques.

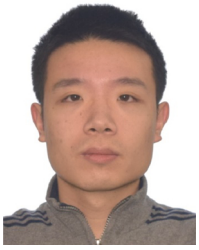

Junjie Li is currently a Ph.D. candidate in Prof. Xueliang (Andy) Sun's Group at the University of Western Ontario, Canada. He received his M.S. degree in physical chemistry from University of Science and Technology of China in 2017. Currently, he is working on the synthesis of advanced nanomaterials for fuel cell applications.

Keegan Adair received his BSc in chemistry from the University of British Columbia in 2016. He is currently a Ph.D. candidate in Prof. Xueliang (Andy) Sun's Nanomaterials and Energy Group at the University of Western Ontario, Canada. Keegan has previous experience in the battery industry through internships at companies including E-One Moli Energy and General Motors R&D. His research interests include the design of nanomaterials for lithium metal batteries and nanoscale interfacial coatings for battery applications.

Yipeng Sun is currently a Ph.D. candidate in Prof. Xueliang (Andy) Sun's Group at the University of Western Ontario, Canada. He is also under the co-supervision of Prof. Tsun-Kong (T.K.) Sham at the University of Western Ontario. He received his B.Eng. degree in Polymer Science and Engineering from Sichuan University (Chengdu, China) in 2016. His research interests focus on the interface modification of electrode materials for lithium-ion batteries.

Ruying Li is a research engineer at Prof. Xueliang (Andy) Sun's Nanomaterial and Energy Group at the University of Western Ontario, Canada. She received her Master degree in Material Chemistry under the supervision of Prof. George Thompson in 1999 at University of Manchester, UK, followed by work as a research assistant under the direction of Prof. Keith Mitchell at the University of British Columbia and under the direction of Prof. Jean-Pol Dodelet at l'Institut national de la recherché scientifique, Canada. Her current research interests are associated with synthesis of nanomaterials for electrochemical energy storage and conversion.

Prof. Meng Gu is a Professor in SUSTech. He received his Ph.D in materials science and engineering from UC Davis. His research focuses on energy-related materials, and development of in-situ TEM and cryo-TEM methods of interface physics and chemistry.

Prof. Zhi-Jian Zhao received his BS and MS degrees in chemistry from Zhejiang University and his Ph.D. degree from Technische Universität München in 2012. After working as a Postdoc with Prof. Greeley in Purdue University, and with Dr Studt and Prof. Nørskov at Stanford University, now he is a professor at Tianjin University. He serves as an Associate Editor for Chemical Engineering Science. His current research focuses on mechanistic studies on heterogeneous catalyst using multi-scaling simulation methods.

Prof. Xueliang Sun is a Canada Research Chair in Development of Nanomaterials for Clean Energy, Fellow of the Royal Society of Canada and Canadian Academy of Engineering and Full Professor at the University of Western Ontario, Canada. Dr. Sun worked as a postdoctoral fellow at the University of British Columbia, Canada and as a Research Associate at L'Institut National de la Recherche Scientifique (INRS), Canada. His current research interests are focused on advanced materials for electrochemical energy storage and conversion, including solid-state batteries, solid-state electrolytes, Li-S batteries, metal-air batteries, single atom catalysts and low temperature fuel cells.